

Ab initio three-loop calculation of the W -exchange contribution to nonleptonic decays of double charm baryons

Thomas Gutsche,¹ Mikhail A. Ivanov,² Jürgen G. Körner,³ Valery E. Lyubovitskij,^{1,4,5,6} and Zhomart Tyulemissov²

¹*Institut für Theoretische Physik, Universität Tübingen,*

Kepler Center for Astro and Particle Physics, Auf der Morgenstelle 14, D-72076 Tübingen, Germany

²*Bogoliubov Laboratory of Theoretical Physics, Joint Institute for Nuclear Research, 141980 Dubna, Russia*

³*PRISMA Cluster of Excellence, Institut für Physik,*

Johannes Gutenberg-Universität, D-55099 Mainz, Germany

⁴*Departamento de Física y Centro Científico Tecnológico de Valparaíso-CCTVal,*

Universidad Técnica Federico Santa María, Casilla 110-V, Valparaíso, Chile

⁵*Department of Physics, Tomsk State University, 634050 Tomsk, Russia*

⁶*Laboratory of Particle Physics, Tomsk Polytechnic University, 634050 Tomsk, Russia*

We have made an ab initio three-loop quark model calculation of the W -exchange contribution to the nonleptonic two-body decays of the doubly charmed baryons Ξ_{cc}^{++} and Ω_{cc}^{+} . The W -exchange contributions appear in addition to the factorizable tree graph contributions and are not suppressed in general. We make use of the covariant confined quark model previously developed by us to calculate the tree graph as well as the W -exchange contribution. We calculate helicity amplitudes and quantitatively compare the tree graph and W -exchange contributions. Finally, we compare the calculated decay widths with those from other theoretical approaches when they are available.

I Introduction

The discovery of the double charm baryon state Ξ_{cc}^{++} by the LHCb Collaboration [1] in the multibody decay mode $(\Lambda_c K^- \pi^+ \pi^+)$ has provided a strong incentive for further theoretical analysis of the weak decays of double charm baryons. The lifetime of the Ξ_{cc}^{++} has been measured to be $(0.256^{+0.024}_{-0.022}(\text{stat}) \pm 0.014(\text{syst}))$ ps [2]. The existence of the Ξ_{cc}^{++} was confirmed in Ref. [3], again by the LHCb Collaboration, who reported on the first observation of a two-body nonleptonic decay of the doubly charmed baryon $\Xi_{cc}^{++} \rightarrow \Xi_c^+ + \pi^+$. In the same report the mass of the Ξ_{cc}^{++} measured in [1] was confirmed.

The nonleptonic two-body decays of baryons have five different color-flavor quark topologies. The set of contributing topological quark diagrams divides into two groups: (i) the reducible tree-diagrams, and (ii) the irreducible W -exchange diagrams. The tree-diagrams are factorized into the lepton decay of the emitted meson and the baryon-baryon transition matrix elements of the weak currents. The W -exchange diagrams are more difficult to evaluate from first principles. First attempts to estimate the W -exchange contributions have been made in [4, 5] using a pole model approach and in [6] using final state interactions based on triangle diagrams describing one-particle exchanges. The authors of [4, 5] and [6] emphasize that their results provide only first estimates of the W -exchange contributions, in particular since their calculations involve generous approximations the errors of which are hard to quantify.

From the work of [4, 5] one knows that the W -exchange contributions to nonleptonic double charm baryon decays are sizeable and cannot be neglected. The W -exchange contributions can interfere destructively or constructively with the tree diagram contributions. It is therefore of utmost importance to get the W -exchange contributions right. In this paper we set out to calculate the W -exchange contributions to the Cabibbo favored nonleptonic two-body decays of double charm baryons. We use the framework of our previously developed covariant constituent quark model to calculate the contributing three-loop quark Feynman diagrams. In a precursor of our present model some of us have calculated nonleptonic charm and bottom baryons including W -exchange contributions [7]. We used a structureless static approximation for the light quark (u, d, s) propagators and the leading-order contribution for the heavy quark (c, b) propagators in the $1/m_{c/b}$ expansion. In the present calculation we use full quark propagators for the light and heavy quarks. We also now include quark confinement in an effective way.

II Decay topologies of Cabibbo favored doubly charmed baryon nonleptonic decays

We begin by a discussion of the different color-flavor topologies that contribute to the nonleptonic two-body transitions of the double heavy Ξ_{cc} and Ω_{cc} states. The relevant topologies are displayed in Fig. 1. We refer to the topologies of Ia and Ib as tree diagrams. They are also sometimes called external (Ia) and internal W -emission (Ib) diagrams. The topologies IIa, IIb, and III are referred to as W -exchange diagrams. The labeling of the topologies follows the labeling

introduced in [8, 9]. In [10] the W -exchange diagrams are denoted as the exchange (IIa), color-commensurate (IIb) and bow tie (III) diagram. The contribution of the various topological diagrams to a particular decay is determined by the quark flavor composition of the particles involved in the decay. For example, the decay $\Xi_{cc}^{++} \rightarrow \Sigma_c^{++} + \bar{K}^{*0}$ proceeds solely via the tree diagram Ib. In [11, 12] this decay has been interpreted as making up a large part of the discovery final state channel ($\Lambda_c^+ K^- \pi^+ \pi^+$) via the decay chain $\Xi_{cc}^{++} \rightarrow \Sigma_c^{++} (\rightarrow \Lambda_c^+ + \pi^+) + \bar{K}^{*0} (\rightarrow K^- + \pi^+)$.

As shown in Fig. 1, the color-flavor factor of the tree diagrams Ia and Ib depend on whether the emitted meson is charged or neutral. For charged emission the color-flavor factor is given by the combination of the Wilson coefficients ($C_2 + \xi C_1$), where $\xi = 1/N_c$ and N_c is the number of colors, while for neutral emission the color-flavor factor reads ($C_1 + \xi C_2$). We take $C_1 = -0.51$ and $C_2 = 1.20$ at $\mu = m_c = 1.3$ GeV from Ref. [13]. We use the large N_c limit for the color-flavor factors. For the W -exchange diagrams the color-flavor factor is given by $(C_2 - C_1)$.

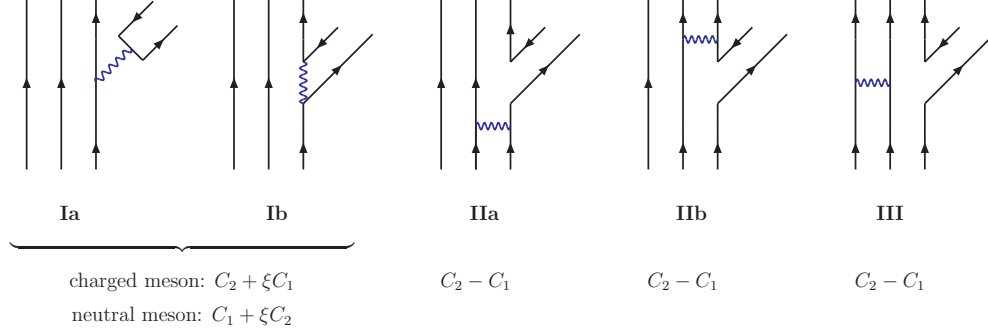


FIG. 1: Flavor-color topologies of nonleptonic weak decays.

The decay of present interest $\Xi_{cc}^{++} \rightarrow \Xi_c^+ + \pi^+$ [3] is fed by the tree diagram Ia and the W -exchange diagram IIb. We treat this decay as well as the seven remaining $1/2^+ \rightarrow 1/2^+ + P(V)$ decays that belong to the same topology class, namely

$$\begin{aligned}
 \Xi_{cc}^{++} &\rightarrow \Xi_c^+ + \pi^+(\rho^+) \\
 \Xi_{cc}^{++} &\rightarrow \Xi_c'^+ + \pi^+(\rho^+) \\
 \Omega_{cc}^+ &\rightarrow \Xi_c^+ + \bar{K}^0(K^{*0}) \\
 \Omega_{cc}^+ &\rightarrow \Xi_c'^+ + \bar{K}^0(K^{*0})
 \end{aligned} \tag{1}$$

The W -exchange contributions to these decays fall into two classes. The first class of these decays involves a $\Xi_c'^+$ -baryon containing a symmetric $\{us\}$ diquark described by the interpolating current $\varepsilon_{abc}(u^b C \gamma_\mu s^c)$, where $C = \gamma^0 \gamma^2$ is the charge conjugation matrix defined in terms of the Dirac matrices. The W -exchange contribution is strongly suppressed due to the Körner, Pati, Woo (KPW) theorem [14, 15]. This theorem states that the contraction of the flavor antisymmetric current-current operator with a flavor symmetric final state configuration is zero in the $SU(3)$ limit. The antisymmetric $[us]$ diquark emerging from the weak vertex is in the 3^* representation and cannot evolve into the 6 representation of the symmetric final state $\{us\}$ diquark. In the following we will calculate $SU(3)$ breaking effects for the W -exchange contributions to this class of decays. The second class involves a Ξ_c^+ -baryon containing a antisymmetric $[us]$ diquark described by the interpolating current $\varepsilon_{abc}(u^b C \gamma_5 s^c)$. In this case the W -exchange contribution is not a priori suppressed. In Table I we display the quantum numbers, mass values, and interpolating currents of double and single charmed baryons needed in this paper.

TABLE I: Quantum numbers and interpolating currents of double and single charmed baryons.

| Baryon | J^P | Interpolating current | Mass (MeV) |
|-----------------|-----------------|--------------------------------------------------------------------|------------|
| Ξ_{cc}^{++} | $\frac{1}{2}^+$ | $\varepsilon_{abc} \gamma^\mu \gamma_5 u^a (c^b C \gamma_\mu c^c)$ | 3620.6 |
| Ω_{cc}^+ | $\frac{1}{2}^+$ | $\varepsilon_{abc} \gamma^\mu \gamma_5 s^a (c^b C \gamma_\mu c^c)$ | 3710.0 |
| $\Xi_c'^+$ | $\frac{1}{2}^+$ | $\varepsilon_{abc} \gamma^\mu \gamma_5 c^a (u^b C \gamma_\mu s^c)$ | 2577.4 |
| Ξ_c^+ | $\frac{1}{2}^+$ | $\varepsilon_{abc} c^a (u^b C \gamma_5 s^c)$ | 2467.9 |

III Matrix elements and decay widths

The effective Hamiltonian describing the $\bar{s}c \rightarrow \bar{u}d$ transition is given by

$$\begin{aligned}\mathcal{H}_{\text{eff}} &= -g_{\text{eff}} (C_1 \mathcal{Q}_1 + C_2 \mathcal{Q}_2) + \text{H.c.}, \\ \mathcal{Q}_1 &= (\bar{s}_a O_L c_b)(\bar{u}_b O_L d_a) = (\bar{s}_a O_L d_a)(\bar{u}_b O_L c_b), \\ \mathcal{Q}_2 &= (\bar{s}_a O_L c_a)(\bar{u}_b O_L d_b) = (\bar{s}_a O_L d_b)(\bar{u}_b O_L c_a),\end{aligned}\quad (2)$$

where we use the notation $g_{\text{eff}} = \frac{G_F}{\sqrt{2}} V_{cs} V_{ud}^\dagger$ and $O_{L/R}^\mu = \gamma^\mu (1 \mp \gamma_5)$ for the weak matrices with left/right chirality.

The nonlocal version of the interpolating currents shown in Table I reads

$$\begin{aligned}J_{B_{cc}}(x) &= \int dx_1 \int dx_2 \int dx_3 F_{B_{cc}}(x; x_1, x_2, x_3) \varepsilon_{a_1 a_2 a_3} \gamma^\mu \gamma_5 q_{a_1}(x_1) (c_{a_2}(x_2) C \gamma_\mu c_{a_3}(x_3)), \\ J_{B_c}(x) &= \int dx_1 \int dx_2 \int dx_3 F_{B_c}(x; x_1, x_2, x_3) \varepsilon_{a_1 a_2 a_3} \Gamma_1 c_{a_1}(x_1) (u_{a_2}(x_2) C \Gamma_2 s_{a_3}(x_3)), \\ F_B &= \delta^{(4)}\left(x - \sum_{i=1}^3 w_i x_i\right) \Phi_B\left(\sum_{i<j}^3 (x_i - x_j)^2\right),\end{aligned}\quad (3)$$

where $q = s$ or u , $w_i = m_i / (\sum_{j=1}^3 m_j)$ and m_i is the quark mass at the space-time point x_i , and Γ_1, Γ_2 are the Dirac strings of the initial and final baryon states as specified in Table I. Here F_B and Φ_B are the Bethe-Salpeter kernel specifying the coupling of baryon with constituent quarks and correlation function, describing the distribution of quarks in baryon, respectively.

The tree diagram and the IIb W -exchange contributions to the matrix element of the nonleptonic decays of the Ξ_{cc}^{++} and Ω_{cc}^+ read

$$\langle B_2 M | \mathcal{H}_{\text{eff}} | B_1 \rangle = g_{\text{eff}} \bar{u}(p_2) \left(12 C_T M_T + 12 (C_1 - C_2) M_W \right) u(p_1). \quad (4)$$

The tree diagram color factor for the neutral Ω_{cc}^+ decays is given by $C_T = -(C_1 + \xi C_2)$ and by $C_T = +(C_2 + \xi C_1)$ for the charged Ξ_{cc}^+ decays. The factor of $\xi = 1/N_c$ is set to zero in our numerical calculations. The overall factor of 12 in Eq. (4) has its origin in a combinatorial factor of 2 and a factor of 6 from the contraction of two Levi-Civita color tensors. The Feynman diagrams describing these processes are depicted in Fig. 2.

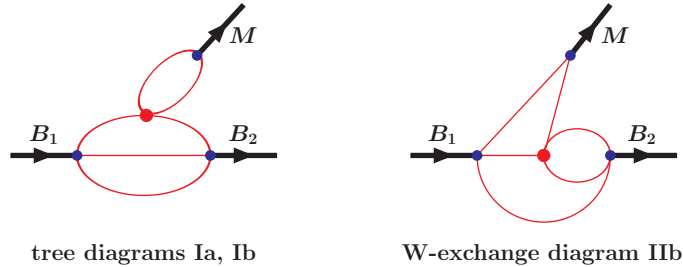


FIG. 2: Pictorial representations of Eqs. (5) and (6).

The contribution from the tree diagram factorizes into two pieces according to

$$\begin{aligned}M_T &= M_T^{(1)} \cdot M_T^{(2)}, \\ M_T^{(1)} &= N_c g_M \int \frac{d^4 k}{(2\pi)^4 i} \tilde{\Phi}_M(-k^2) \text{tr} [O_L^\delta S_d(k - w_d q) \Gamma_M S_{s(u)}(k + w_{s(u)} q)] \\ M_T^{(2)} &= g_{B_1} g_{B_2} \int \frac{d^4 k_1}{(2\pi)^4 i} \int \frac{d^4 k_2}{(2\pi)^4 i} \tilde{\Phi}_{B_1}(-\vec{\Omega}_1^2) \tilde{\Phi}_{B_2}(-\vec{\Omega}_2^2) \\ &\quad \times \Gamma_1 S_c(k_2) \gamma^\mu S_c(k_1 - p_1) O_R \delta S_{u(s)}(k_1 - p_2) \tilde{\Gamma}_2 S_{s(u)}(k_1 - k_2) \gamma_\mu \gamma_5.\end{aligned}\quad (5)$$

Here $\Gamma_1 \otimes \tilde{\Gamma}_2 = +I \otimes \gamma_5$ for the Ξ_c^+ -baryon and $-\gamma_\nu \gamma_5 \otimes \gamma^\nu$ for the $\Xi_c'^+$ -baryon.

The coupling constants g_M , g_{B_1} and g_{B_2} are determined as described in our previous papers (for details see, e.g. [11, 16]). The Dirac matrix Γ_M in $M_T^{(1)}$ reads γ_5 and $\epsilon_V \cdot \gamma$ for the pseudoscalar meson P and for the vector meson V . The connection of $M_T^{(1)}$ with the leptonic decay constants $f_M = f_P, f_V$ is given by $M_T^{(1)} = -f_P q^\delta$ and $+f_V m_V \epsilon_V^\delta$. The minus sign in front of f_P appears because the momentum q flows in the opposite direction from the decay of P -meson. The Fourier-transforms of the vertex functions described by the nonlocal interpolating currents are denoted by $\tilde{\Phi}_H$. We use for them the Gaussian functional form: $\tilde{\Phi}_H(-k^2) = \exp(k^2/\Lambda_H^2)$, where Λ_H is the hadron size parameter. Here and in the following the arguments of the baryonic vertex functions are expressed through the Jacobi momenta (q_1, q_2) and (r_1, r_2) by $\vec{\Omega}_1^2 = \frac{1}{2}(q_1 + q_2)^2 + \frac{1}{6}(q_1 - q_2)^2$, $\vec{\Omega}_2^2 = \frac{1}{2}(r_1 + r_2)^2 + \frac{1}{6}(r_1 - r_2)^2$. The momenta q_i and r_i are defined from momenta conservation in each vertex of the diagrams (see details in Ref. [11, 16]).

The calculation of the three-loop W -exchange contribution is much more involved because the matrix element does not factorize. By using the Fierz transformation $O_{L/R}^{\alpha_1\alpha_2} O_{R/L}^{\alpha_3\alpha_4} = 2(1 \pm \gamma_5)^{\alpha_1\alpha_4} (1 \mp \gamma_5)^{\alpha_3\alpha_2}$ one has

$$\begin{aligned} M_W &= g_{B_1} g_{B_2} g_M \int \frac{d^4 k_1}{(2\pi)^4 i} \int \frac{d^4 k_2}{(2\pi)^4 i} \int \frac{d^4 k_3}{(2\pi)^4 i} \tilde{\Phi}_{B_1}(-\vec{\Omega}_1^2) \tilde{\Phi}_{B_2}(-\vec{\Omega}_2^2) \tilde{\Phi}_M(-P^2) \\ &\times 2 \Gamma_1 S_c(k_1) \gamma^\mu S_c(k_2) (1 - \gamma_5) S_d(k_2 - k_1 + p_2) \Gamma_M S_{s(u)}(k_2 - k_1 + p_1) \gamma_\mu \gamma_5 \\ &\times \text{tr} \left[S_{u(s)}(k_3) \tilde{\Gamma}_2 S_{s(u)}(k_3 - k_1 + p_2) (1 + \gamma_5) \right], \end{aligned} \quad (6)$$

where $\Gamma_1 \otimes \tilde{\Gamma}_2 = I \otimes \gamma_5$ for $B_2 = \Xi_c^+$ and $-\gamma_\nu \gamma_5 \otimes \gamma^\nu$ for $B_2 = \Xi_c'^+$. Here $P = k_2 - k_1 + w_d p_1 + w_u p_2$ is the Jacobi momentum in the meson vertex function.

We are now in the position to verify the KPW theorem in our three-loop calculation. To do this, we change the order of Dirac matrices in the trace by using the properties of the charge conjugation matrix. Keeping in mind that γ_5 does not contribute to the trace, we have

$$\text{tr} \left[S_u(k_3) \gamma_\nu S_s(k_3 - k_1 + p_2) \right] = -\text{tr} \left[S_s(-k_3 + k_1 - p_2) \gamma_\nu S_u(-k_3) \right]. \quad (7)$$

We insert Eq. (7) into Eq. (6) and shift the integration variable $k_3 \rightarrow -k_3 + k_1 - p_2$. One can check that $\vec{\Omega}_2^2$ goes into itself under this transformation accompanied by an interchange of the u - and s - quark masses. Thus, if $m_u = m_s$ then M_W is identical zero which directly confirms the KPW-theorem. We have checked numerically that the three-loop integral vanishes in this limit.

Details of the calculation of the loop integrals and the subsequent reduction of the integration over Fock-Schwinger variables to an integration over a hypercube may be found in our previous papers (see e.g. the most recent papers [11, 16]). Compared to the two-loop calculation of [11, 16] we are now dealing with a three-loop calculation involving six quark propagators instead of the four propagators in the two-loop case. The calculation is quite time-consuming both analytically and numerically.

Next one expands the transition amplitudes in terms of invariant amplitudes. One has

$$\langle B_2 P | \mathcal{H}_{\text{eff}} | B_1 \rangle = g_{\text{eff}} \bar{u}(p_2) (A + \gamma_5 B) u(p_1), \quad (8)$$

$$\langle B_2 V | \mathcal{H}_{\text{eff}} | B_1 \rangle = g_{\text{eff}} \bar{u}(p_2) \epsilon_{V\delta}^* (\gamma^\delta V_\gamma + p_1^\delta V_p + \gamma_5 \gamma^\delta V_{5\gamma} + \gamma_5 p_1^\delta V_{5p}) u(p_1). \quad (9)$$

The invariant amplitudes are converted to a set of helicity amplitudes $H_{\lambda_1 \lambda_M}$ as described in [8]. One has

$$\begin{aligned} H_{\frac{1}{2}t}^V &= \sqrt{Q_+} A, & H_{\frac{1}{2}t}^A &= \sqrt{Q_-} B, \\ H_{\frac{1}{2}0}^V &= +\sqrt{Q_-/q^2} \left(m_+ V_\gamma + \frac{1}{2} Q_+ V_p \right), & H_{\frac{1}{2}1}^V &= -\sqrt{2Q_-} V_\gamma, \\ H_{\frac{1}{2}0}^A &= +\sqrt{Q_+/q^2} \left(m_- V_{5\gamma} + \frac{1}{2} Q_- V_{5p} \right), & H_{\frac{1}{2}1}^A &= -\sqrt{2Q_+} V_{5\gamma}, \end{aligned} \quad (10)$$

where $m_\pm = m_1 \pm m_2$, $Q_\pm = m_\pm^2 - q^2$ and $|\mathbf{p}_2| = \lambda^{1/2}(m_1^2, m_2^2, q^2)/(2m_1)$. The helicities of the three particles are related by $\lambda_1 = \lambda_2 - \lambda_M$. We use the notation $\lambda_P = \lambda_t = 0$ for the scalar ($J = 0$) contribution in order to set the helicity label apart from $\lambda_V = 0$ used for the longitudinal component of the $J = 1$ vector meson. The remaining helicity amplitudes can be obtained from the parity relations $H_{-\lambda_2, -\lambda_M}^V = +H_{\lambda_2, \lambda_M}^V$ and $H_{-\lambda_2, -\lambda_M}^A = -H_{\lambda_2, \lambda_M}^A$. The helicity amplitudes have the dimension $[m]^3$. The numerical results on the helicity amplitudes given in Tables II-V are in units of GeV^3 .

The two-body decay widths read

$$\Gamma(B_1 \rightarrow B_2 + P) = \frac{g_{\text{eff}}^2 |\mathbf{p}_2|}{16\pi m_1^2} \mathcal{H}_S, \quad \mathcal{H}_S = \left| H_{\frac{1}{2}t} \right|^2 + \left| H_{-\frac{1}{2}t} \right|^2, \quad (11)$$

$$\Gamma(B_1 \rightarrow B_2 + V) = \frac{g_{\text{eff}}^2 |\mathbf{p}_2|}{16\pi m_1^2} \mathcal{H}_V, \quad \mathcal{H}_V = \left| H_{\frac{1}{2}0} \right|^2 + \left| H_{-\frac{1}{2}0} \right|^2 + \left| H_{\frac{1}{2}1} \right|^2 + \left| H_{-\frac{1}{2}1} \right|^2, \quad (12)$$

where we denote the sum of the squared moduli of the helicity amplitudes $H = H^V - H^A$ by \mathcal{H}_S and \mathcal{H}_V [16].

IV Numerical results

All model parameters have been fixed in our previous studies except for the size parameter Λ_{cc} of the double charmed baryons. As a first approximation we equate the size parameter of double charm baryons with that of single charm baryons, i.e. we take $\Lambda_{cc} = \Lambda_c = 0.8675$ GeV where we adopt the value of Λ_c from [17]. Numerical results for the helicity amplitudes and decay widths are displayed in the Tables II-V. In this paper we concentrate on our predictions for rate values. On top of the rate predictions, Tables II-V contain a wealth of spin polarization information. For example, for the decay $\Xi_{cc}^{++} \rightarrow \Xi_c^+ + \pi^+$ one finds an asymmetry parameter of $\alpha = -2H_{1/20}^V H_{1/20}^A / (|H_{1/20}^V|^2 + |H_{1/20}^A|^2) = -0.57$ while [4] predict a value in the range $\alpha = [-0.86, -1.00]$ depending on their model assumptions. Note that the W -exchange contribution in [4] is purely p -wave, i.e. proportional to $H_{1/20}^A$, due to the nonrelativistic approximations that they employ. This is in stark contrast to our relativistic result where the s -wave amplitude dominates in this process, i.e. $H_{1/20}^V/H_{1/20}^A = 3.3$. Both model calculations agree on a very substantial destructive interference of the tree and W -exchange contributions.

Our results highlight the importance of the KPW theorem for the nonleptonic decays when the final state involves a Ξ'^+ baryon containing a symmetric $\{su\}$ diquark. Tables II-V show that the relevant W -exchange contributions are strongly suppressed. Nonzero values result from $SU(3)$ breaking effects which are accounted for in our approach. Take for example the decay $\Xi_{cc}^{++} \rightarrow \Xi_c'^+ + \pi^+$. When compared to the tree contribution the $SU(3)$ breaking effects amount to $\sim (2 - 4)\%$. While the consequences of the KPW theorem for the W -exchange contribution are incorporated in the pole model approach of [4] they are not included in the final-state interaction approach of [6].

In Table VI we compare our rate results with the results of some other approaches [4–6, 12, 18, 19]. Note that the rates calculated in [18] include tree graph contributions only. There is a wide spread in the rate values predicted by the various model calculations. All calculations approximately agree on the rate of the decay $\Xi_{cc}^{++} \rightarrow \Xi_c'^+ + \rho^+$ which is predicted to have a large branching ratio of $\sim 16\%$. In our calculation this mode is predicted to have by far the largest branching ratio of the decays analyzed in this paper. As concerns the decay $\Xi_{cc}^{++} \rightarrow \Xi_c^+ + \pi^+$ discovered by the LHCb Collaboration [3] we find a branching ratio of $\mathcal{B}(\Xi_{cc}^{++} \rightarrow \Xi_c^+ \pi^+) = 0.70\%$ using the central value of the life time measurement in [2]. The small value of the branching ratio results from a substantial cancellation of the tree and W -exchange contributions. The branching ratio is somewhat smaller than the branching ratio $\mathcal{B}(\Xi_{cc}^{++} \rightarrow \Sigma_c^{++} + \bar{K}^0) = 1.28\%$ calculated in [11]. We predict a branching ratio considerably smaller than the range of branching fractions $(6.66 - 15.79)\%$ calculated in [4].

An important issue is the accuracy of our results. The only free parameter in our approach is the size parameter Λ_{cc} of the double heavy baryons for which we have chosen $\Lambda_{cc} = 0.8675$ GeV in Tables II-V. In order to estimate the uncertainty caused by the choice of the size parameter we allow the size parameter to vary from 0.6 to 1.135 GeV. We evaluate the mean $\bar{\Gamma} = \sum \Gamma_i / N$ and the mean square deviation $\sigma^2 = \sum (\Gamma_i - \bar{\Gamma})^2 / N$. The results for $N = 5$ are shown in Table VII. The rate errors amount to 6 – 15%. Since the dependence of the rates on Λ_{cc} is nonlinear the central values of the rates in Table VII do not agree with the rate values in Tables II-V.

V Outlook

We now have the tools at hand to calculate all Cabibbo favored and Cabibbo suppressed nonleptonic two-body decays of the double charm ground state baryons Ξ_{cc}^{++} , Ξ_{cc}^+ , and Ω_{cc}^+ . These would also include the $1/2^+ \rightarrow 3/2^+ + P(V)$ nonleptonic decays not treated in this paper. Of particular interest are the modes $\Xi_{cc}^+ \rightarrow \Sigma^{(*)+} + D^{(*)0}$ (III), $\Xi_{cc}^+ \rightarrow \Xi^{(*)0} + D_s^{(*)+}$ (III), and $\Omega_{cc}^+ \rightarrow \Xi^{(*)0} + D^{(*)+}$ (IIb) which are only fed by a single W -exchange contribution as indicated in appendices. Of these the three modes involving the final state $3/2^+$ baryons Σ^{*+} and Ξ^{*0} would be forbidden due to the KPW theorem. It would be interesting to check on this prediction of the quark model.

Acknowledgments

This work was funded by the Carl Zeiss Foundation under Project “Kepler Center für Astro- und Teilchenphysik: Hochsensitive Nachweistechnik zur Erforschung des unsichtbaren Universums (Gz: 0653-2.8/581/2)”, by CONICYT (Chile) PIA/Basal FB0821, by the Russian Federation program “Nauka” (Contract No. 0.1764.GZB.2017), by Tomsk State University competitiveness improvement program (Grant No. 8.1.07.2018), and by Tomsk Polytechnic University Competitiveness Enhancement Program (Grant No. VIU-FTI-72/2017). M.A.I. acknowledges the support from the PRISMA Cluster of Excellence (Mainz Uni.).

TABLE II: $\Omega_{cc}^+ \rightarrow \Xi_c'^+ + \bar{K}^0(\bar{K}^{*0})$

| Helicity | Tree diagram | W diagram | total |
|-----------------------------------------------------------------------------------------------|--------------|-----------------------|-------|
| $H_{\frac{1}{2}t}^V$ | 0.20 | -0.01 | 0.19 |
| $H_{\frac{1}{2}t}^A$ | 0.25 | -0.01 | 0.24 |
| $\Gamma(\Omega_{cc}^+ \rightarrow \Xi_c'^+ + \bar{K}^0) = 0.15 \cdot 10^{-13} \text{ GeV}$ | | | |
| $H_{\frac{1}{2}0}^V$ | -0.25 | 0.04×10^{-1} | -0.25 |
| $H_{\frac{1}{2}0}^A$ | -0.50 | 0.01 | -0.49 |
| $H_{\frac{1}{2}1}^V$ | 0.27 | -0.01 | 0.26 |
| $H_{\frac{1}{2}1}^A$ | 0.56 | 0.04×10^{-2} | 0.56 |
| $\Gamma(\Omega_{cc}^+ \rightarrow \Xi_c'^+ + \bar{K}^{*0}) = 0.74 \cdot 10^{-13} \text{ GeV}$ | | | |

TABLE IV: $\Xi_{cc}^{++} \rightarrow \Xi_c'^+ + \pi^+(\rho^+)$

| Helicity | Tree diagram | W diagram | total |
|-----------------------------------------------------------------------------------------|--------------|-----------------------|-------|
| $H_{\frac{1}{2}t}^V$ | -0.38 | -0.01 | -0.39 |
| $H_{\frac{1}{2}t}^A$ | -0.55 | -0.02 | -0.57 |
| $\Gamma(\Xi_{cc}^{++} \rightarrow \Xi_c'^+ + \pi^+) = 0.82 \cdot 10^{-13} \text{ GeV}$ | | | |
| $H_{\frac{1}{2}0}^V$ | 0.60 | 0.04×10^{-1} | 0.61 |
| $H_{\frac{1}{2}0}^A$ | 1.20 | 0.01 | 1.21 |
| $H_{\frac{1}{2}1}^V$ | -0.49 | -0.01 | -0.50 |
| $H_{\frac{1}{2}1}^A$ | -1.27 | 0.01×10^{-1} | -1.27 |
| $\Gamma(\Xi_{cc}^{++} \rightarrow \Xi_c'^+ + \rho^+) = 4.27 \cdot 10^{-13} \text{ GeV}$ | | | |

TABLE III: $\Omega_{cc}^+ \rightarrow \Xi_c^+ + \bar{K}^0(\bar{K}^{*0})$

| Helicity | Tree diagram | W diagram | total |
|----------------------------------------------------------------------------------------------|--------------|-----------|-------|
| $H_{\frac{1}{2}t}^V$ | -0.35 | 1.06 | 0.71 |
| $H_{\frac{1}{2}t}^A$ | -0.10 | 0.31 | 0.21 |
| $\Gamma(\Omega_{cc}^+ \rightarrow \Xi_c^+ + \bar{K}^0) = 0.95 \cdot 10^{-13} \text{ GeV}$ | | | |
| $H_{\frac{1}{2}0}^V$ | 0.50 | -0.69 | -0.19 |
| $H_{\frac{1}{2}0}^A$ | 0.18 | -0.45 | -0.27 |
| $H_{\frac{1}{2}1}^V$ | -0.11 | -0.24 | -0.35 |
| $H_{\frac{1}{2}1}^A$ | -0.18 | 0.66 | 0.48 |
| $\Gamma(\Omega_{cc}^+ \rightarrow \Xi_c^+ + \bar{K}^{*0}) = 0.62 \cdot 10^{-13} \text{ GeV}$ | | | |

TABLE V: $\Xi_{cc}^{++} \rightarrow \Xi_c^+ + \pi^+(\rho^+)$

| Helicity | Tree diagram | W diagram | total |
|----------------------------------------------------------------------------------------|--------------|-----------|-------|
| $H_{\frac{1}{2}t}^V$ | -0.70 | 0.99 | 0.29 |
| $H_{\frac{1}{2}t}^A$ | -0.21 | 0.30 | 0.09 |
| $\Gamma(\Xi_{cc}^{++} \rightarrow \Xi_c^+ + \pi^+) = 0.18 \cdot 10^{-13} \text{ GeV}$ | | | |
| $H_{\frac{1}{2}0}^V$ | 1.17 | -0.70 | 0.47 |
| $H_{\frac{1}{2}0}^A$ | 0.45 | -0.44 | 0.003 |
| $H_{\frac{1}{2}1}^V$ | -0.20 | -0.23 | -0.43 |
| $H_{\frac{1}{2}1}^A$ | -0.41 | 0.62 | 0.21 |
| $\Gamma(\Xi_{cc}^{++} \rightarrow \Xi_c^+ + \rho^+) = 0.63 \cdot 10^{-13} \text{ GeV}$ | | | |

TABLE VI: Comparison with other approaches. Abbreviation: M=NRQM, T=HQET

| Mode | Width (in 10^{-13} GeV) | | | | | |
|-----------------------------------------------------|------------------------------------|----------------------|------------------------|-----------|---------|--------------|
| | our | Dhir [4, 5] | Jiang [6] | Wang [18] | Yu [12] | Kiselev [19] |
| $\Omega_{cc}^+ \rightarrow \Xi_c'^+ + \bar{K}^0$ | 0.15 | 0.31 (M) 0.59 (T) | | | | |
| $\Omega_{cc}^+ \rightarrow \Xi_c^+ + \bar{K}^0$ | 0.95 | 0.68 (M) 1.08 (T) | | | | |
| $\Omega_{cc}^+ \rightarrow \Xi_c'^+ + \bar{K}^{*0}$ | 0.74 | | $2.64^{+2.72}_{-1.79}$ | | | |
| $\Omega_{cc}^+ \rightarrow \Xi_c^+ + \bar{K}^{*0}$ | 0.62 | | $1.38^{+1.49}_{-0.95}$ | | | |
| $\Xi_{cc}^{++} \rightarrow \Xi_c'^+ + \pi^+$ | 0.82 | 1.40 (M) 1.93 (T) | | 1.10 | | |
| $\Xi_{cc}^{++} \rightarrow \Xi_c^+ + \pi^+$ | 0.18 | 1.71 (M) 2.39 (T) | | 1.57 | 1.58 | 2.25 |
| $\Xi_{cc}^{++} \rightarrow \Xi_c'^+ + \rho^+$ | 4.27 | | $4.25^{+0.32}_{-0.19}$ | 4.12 | 3.82 | |
| $\Xi_{cc}^{++} \rightarrow \Xi_c^+ + \rho^+$ | 0.63 | | $4.11^{+1.37}_{-0.86}$ | 3.03 | 2.76 | 6.70 |

TABLE VII: Estimating uncertainties in the decay widths.

| Mode | Width (in 10^{-13} GeV) |
|----------------------------------------------------|------------------------------------|
| $\Omega_{cc}^+ \rightarrow \Xi_c'^+ + \bar{K}^0$ | 0.14 ± 0.01 |
| $\Omega_{cc}^+ \rightarrow \Xi_c^+ + \bar{K}^0$ | 0.72 ± 0.06 |
| $\Omega_{cc}^+ \rightarrow \Xi_c^+ + \bar{K}^0$ | 0.87 ± 0.13 |
| $\Omega_{cc}^+ \rightarrow \Xi_c^+ + \bar{K}^{*0}$ | 0.58 ± 0.07 |
| $\Xi_{cc}^{++} \rightarrow \Xi_c'^+ + \pi^+$ | 0.77 ± 0.05 |
| $\Xi_{cc}^{++} \rightarrow \Xi_c'^+ + \rho^+$ | 4.08 ± 0.29 |
| $\Xi_{cc}^{++} \rightarrow \Xi_c^+ + \pi^+$ | 0.16 ± 0.02 |
| $\Xi_{cc}^{++} \rightarrow \Xi_c^+ + \rho^+$ | 0.59 ± 0.04 |

-
- [1] R. Aaij *et al.* (LHCb Collaboration), Phys. Rev. Lett. **119**, 112001 (2017).
 - [2] R. Aaij *et al.* (LHCb Collaboration), Phys. Rev. Lett. **121**, 052002 (2018).
 - [3] R. Aaij *et al.* (LHCb Collaboration), Phys. Rev. Lett. **121**, 162002 (2018).
 - [4] N. Sharma and R. Dhir, Phys. Rev. D **96**, 113006 (2017).
 - [5] R. Dhir and N. Sharma, Eur. Phys. J. C **78**, 743 (2018).
 - [6] L. J. Jiang, B. He and R. H. Li, Eur. Phys. J. C **78**, 961 (2018).
 - [7] M. A. Ivanov, J. G. Körner, V. E. Lyubovitskij and A. G. Rusetsky, Phys. Rev. D **57**, 5632 (1998); Mod. Phys. Lett. A **13**, 181 (1998).
 - [8] J. G. Körner and M. Krämer, Z. Phys. C **55**, 659 (1992).
 - [9] J. G. Körner, M. Krämer and D. Pirjol, Prog. Part. Nucl. Phys. **33**, 787 (1994).
 - [10] A. K. Leibovich, Z. Ligeti, I. W. Stewart and M. B. Wise, Phys. Lett. B **586**, 337 (2004).
 - [11] T. Gutsche, M. A. Ivanov, J. G. Körner and V. E. Lyubovitskij, Phys. Rev. D **96**, 054013 (2017).
 - [12] F. S. Yu, H. Y. Jiang, R. H. Li, C. D. Lü, W. Wang and Z. X. Zhao, Chin. Phys. C **42**, 051001 (2018).
 - [13] G. Buchalla, A. J. Buras and M. E. Lautenbacher, Rev. Mod. Phys. **68**, 1125 (1996).
 - [14] J. G. Körner, Nucl. Phys. **B25**, 282 (1971).
 - [15] J. C. Pati and C. H. Woo, Phys. Rev. D **3**, 2920 (1971).
 - [16] T. Gutsche, M. A. Ivanov, J. G. Körner and V. E. Lyubovitskij, Phys. Rev. D **98**, 074011 (2018); T. Gutsche, M. A. Ivanov, J. G. Körner, V. E. Lyubovitskij, V. V. Lyubushkin and P. Santorelli, Phys. Rev. D **96**, 013003 (2017).
 - [17] T. Gutsche, M. A. Ivanov, J. G. Körner, V. E. Lyubovitskij and P. Santorelli, Phys. Rev. D **93**, 034008 (2016).
 - [18] W. Wang, F. S. Yu and Z. X. Zhao, Eur. Phys. J. C **77**, 781 (2017).
 - [19] V. V. Kiselev and A. K. Likhoded, Phys. Usp. **45**, 455 (2002) [Usp. Fiz. Nauk **172**, 497 (2002)]; A. V. Berezhnoy, A. K. Likhoded and A. V. Luchinsky, Phys. Rev. D **98**, 113004 (2018).